Magnetohydromagnetic Stagnation Point-Flow of Micropolar fluids Past a Permeable Stretching Plate in Porous Media with Thermal Radiation, Chemical Reaction and Viscous Dissipation

E. O. [1] **Fatunmbi**, **A.** [2] **Adeniyan**.

[1] Department of mathematics and Statistics, Federal Polytechnic, Ilaro, Ogun State, Nigeria.

[1] E-mail: olusojiephesus@yahoo.com

[2] Department of Mathematics, University of Lagos, Akoka, Lagos State, Nigeria.

[2] E-mail: aadeniyan@unilag.edu.ng

Abstract

The study investigates the steady two-dimensional, stagnation point, heat and mass transfer of an incompressible, electrically conducting micropolar fluid flow past a permeable stretching plate in a Darcy-Forchheimer porous medium. The presence of thermal radiation, chemical reaction, viscous dissipation, heat source/sink and variable thermal conductivity are examined. The governing partial differential equations of the fluid flow are transformed into non-linear ordinary differential equations using similarity variables. The resulting equations are solved by fourth order Runge-Kutta integration scheme alongside shooting method. Furthermore, the effects of embedded governing parameters on the dimensionless velocity, temperature, microrotation and concentration profiles are presented graphically. Similarly, the influences of the physical flow parameters on the Skin friction, Nusselt number, Sherwood and Wall couple stress are examined and presented in tables. Comparison of the present results with the published results in the literature in some limiting situations shows a perfect agreement.

Keywords: Magnetohydrodynamic flow; Micropolar fluid; Porous medium; Stagnation point; Stretching plate.

1. Introduction

The increasing significance of non-Newtonian fluids in the engineering and manufacturing processes has boosted researchers and engineers interest in studying the characteristics and behaviour of such types of fluid under various situations and geometries. These fluids are particularly important in real industrial applications, such as in polymer engineering, crude oil extraction, food processing, to mention but a few. However, as a result of diverse fluid characteristics, in nature, all the non-Newtonian fluids cannot be explained by a single constitutive model. It has been observed that the Navier-Stokes equations of classical hydrodynamic can not adequately describe the rheological characteristics of complex fluids of industrial significance. These have led to the development of various kinds of non-Newtonian fluid models depending on different physical characteristics such as: Casson fluid, Jeffery fluid, Maxwell fluid, Johnson-Segalman fluid, Ostwald De-Waele power law fluid, Micropolar fluid a few of many (Chen *et al.*, 2011).

The experiment carried out by Holt and Fabula (1964), Vogel and Patterson (1964) on fluids with small amount of polymeric additives shows that fluids with additives manifest a reduction in skin friction near a rigid body. This phenomenon can neither be captured nor explained by the Newtonian fluid mechanics. Eringen (1966, 1972) initiated the theory of micropolar fluids and as well derived the constitutive equations for the theory of thermo-micropolar fluids. These are fluids with microstructure which constitute a substantial generalization of the Navier-Stokes model and opens up a new field of potentials application. By this theory, each element of the fluid is

associated to two sets of degrees of freedom: (a) translatory degrees of freedom, giving rise to velocity, and (b) rotation and stretch, allowing the particles to undergo independent intrinsic spins and homogenous deformation (Eringen, 1972).

The concept of micropolar fluid deals with a class of fluids that exhibit certain microscopic effect arising from the local structure and micromotion of the fluid element. Examples of micropolar fluids are: polymeric fluids, fluid suspensions, animal blood, liquid crystals, colloidal fluids, clouds with dust (Ahmadi, 1976; Hayat *et al.*, 2011). A detailed review, on the theory and applications of micropolar fluids, was given by Lukaszewicz (1999). The boundary layer flow of such fluids was first studied by Peddieson and McNitt (1970) and Wilson (1970).

The flow and heat transfer over stretching surfaces find practical applications in technological processes such as extrusion of plastic sheet, glass blowing, artificial fibers and polymeric sheets, heat materials traveling between a feed roll, textile and paper production (Khan *et al,2015*). The pioneering work on stretching sheet was done by Crane (1970) and extended by Gupta and Gupta (1977) to include heat and mass transfer on stretching sheet with suction or blowing. Recently, Mishra *et al.*, (2016) numerically studied chemical reaction and Soret effects on hydromagnetic micropolar fluid along a stretching sheet. The authors found that flow reversal occur for microrotation in the presence of inertial coefficient and porosity of the medium. The imposition of magnetic field on the study of flow and heat transfer past stretching plate has motivated researchers due to its practical applications in areas such as hot rolling, the extrusion of polymer sheet from a die, the cooling of metallic sheets. In such processes, the properties of the end products depend on the kinematic of stretching and the rate of cooling. The rate of cooling can be controlled by drawing the sheets in an electrically conducting fluid subjected to a magnetic field (Mukhopadhyay, 2013.)

The flow and heat transfer in an electrically conducting micropolar fluids past a porous plate under the influence of a magnetic field has also been examined by researchers owing to its applications in engineering devices such as MHD generators, geothermal energy extractions, nuclear reactors/burial of nuclear wastes and boundary layer control in the field of aerodynamics (Pal and Chatterjee, 2010; Mahmoud, 2011).

In practice, it has been found that porous medium and the variation of fluid viscosity have a remarkable influence on the flow field as well as the temperature field of a fluid of nonnegligible thermal dissipation. For instance, a decrease in fluid viscosity can make the fluid velocity decrease appreciably with an increase in transverse distance from a stretching plate (Mukhopadhyay *et al.*, 2005). Furthermore, thermal radiation effects become important when there is occurrence of high temperature difference between the surface and the ambient temperature. Such study is found useful in building relevant equipment in engineering applications such as in nuclear reactors, electric power generation and solar power technology (Mukhopadhyay, 2013; Dar and Elangovan, 2016 and 2017).

Stagnation point flow occurs when the fluid flow impinges on a solid object, the fluid velocity at such point is relatively zero. Such study has attracted many scholars due to its practical applications such as extrusion of polymers in melt-spinning processes, the cooling of nuclear reactors during emergency shut down and cooling of electronic devices. Mahapatra and Gupta (2002) investigated the flow and heat transfer characteristics over a stretching sheet with a uniform magnetic field and prescribed surface heat flux. Jat *et al., 2012* investigated MHD stagnation point flow and heat transfer of a micropolar fluid in a porous medium. However, these authors ignore the mass transfer effect. Ibrahim and Suneetha (2015) examined the effects of heat generation and thermal radiation on steady MHD flow near a stagnation point on a linear stretching sheet in a porous medium with mass transfer. However, the influences of chemical reaction, viscous dissipation and

suction/injection on non-Newtonian micropolar fluid were not considered inspite of their physical importance. Pandey and Kumar (2016) inspected the effect of viscous dissipation and suction/injection on MHD nano fluid flow over a wedge with porous medium and slip.

The aim of this study is to investigate the MHD stagnation-point flow of micropolar fluids past permeable stretching plate in porous media with the influences of thermal radiation, chemical reaction and viscous dissipation and variable thermal conductivity. Using similarity transformations, the governing equations are converted into nonlinear ordinary equations and then solved numerically by the means of shooting method with fourth order Runge-Kutta method.

2. Formulation of the Problem

Consider a steady two-dimensional flow of viscous, incompressible electrically conducting micropolar fluid past a permeable stretching plate in a saturated porous medium towards a stagnation point. A uniform magnetic field of strength B_o is applied normal to the direction of flow in which (x, y) depicts the stretching and the transverse coordinates with corresponding velocity component (u, v) respectively. Two equal and opposing forces are introduced along the stretching axis such that the plate is stretched keeping the origin fixed at $y = 0$ as depicted in Fig. 1 and fluid occupies $y \geq 0$. The stretching velocity u_w and the free stream velocity U_∞ are assumed to vary proportional to the distance x measured from the stagnation point o, i.e. $u_w = ax$ and $u_\infty = bx$, where a is a positive constant and b is a non-negative positive constant, the plate is maintained at a constant temperature T_w. The fluid properties are isotropic and constant except the density variation with temperature and concentration in the body force term and the fluid thermal conductivity which vary linearly with temperature. It is assumed also that the magnetic Reynolds number is small such that the induced magnetic field is negligible as compared to the applied magnetic field. In addition, the fluid is assumed to be gray emitting and absorbing but not scattering and the optically thick radiative flux is simplified using the Rosseland approximation. Under the above assumptions and the boundary layer approximations, the governing equations of the fluid flow are:

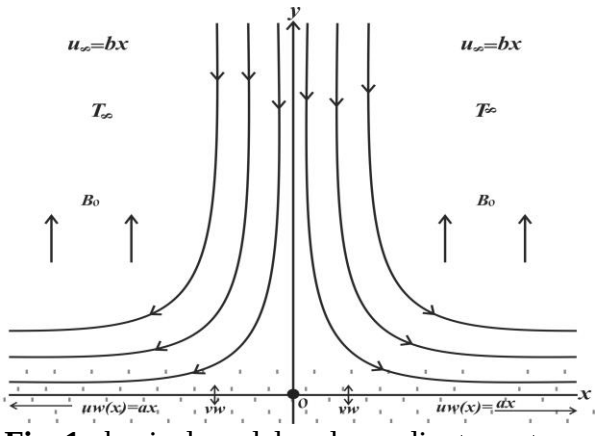

Fig. 1 physical model and coordinate system

$$\frac{\partial u}{\partial x}+\frac{\partial v}{\partial y}=0, \tag{1}$$

$$u\frac{\partial u}{\partial x}=-\frac{1}{\rho}\frac{\partial p}{\partial x}+\frac{(\mu+\kappa)}{\rho}\frac{\partial^2 u}{\partial y^2}+\frac{\kappa}{\rho}\frac{\partial N}{\partial y}-\frac{\sigma B_o^2}{\rho}u-\frac{\nu}{K_p}u-\frac{F}{K_p}u^2, \tag{2}$$

where

$$u_\infty\frac{du}{dx}=-\frac{1}{\rho}\frac{\partial p}{\partial x}-\frac{\sigma B_o^2}{\rho}u-\frac{\nu}{K_p}u-\frac{F}{K_p}u^2, \tag{3}$$

using eq. (3) in (2) gives

$$u\frac{\partial u}{\partial x}=u_\infty\frac{du_\infty}{dx}+\frac{(\mu+\kappa)}{\rho}\frac{\partial^2 u}{\partial y^2}+\frac{\kappa}{\rho}\frac{\partial N}{\partial y}-\frac{\sigma B_o^2}{\rho}(u-u_\infty)-\frac{\nu}{K_p}(u-u_\infty)-\frac{F}{K_p}\left(u^2-u_\infty^2\right), \tag{4}$$

$$u\frac{\partial N}{\partial x}+v\frac{\partial N}{\partial y}=\frac{\gamma}{\rho j}\frac{\partial^2 N}{\partial y^2}-\frac{\kappa}{\rho j}\left(2N+\frac{\partial u}{\partial y}\right), \tag{5}$$

$$u\frac{\partial T}{\partial x}+v\frac{\partial T}{\partial y}=\frac{1}{\rho C_p}\frac{\partial}{\partial y}\left(k(T)\frac{\partial T}{\partial y}\right)+\frac{\mu+\kappa}{\rho C_p}\left(\frac{\partial u}{\partial y}\right)^2-\frac{1}{\rho C_p}\frac{\partial q_r}{\partial y}+\frac{q}{\rho c_p}(T-T_\infty), \tag{6}$$

$$u\frac{\partial C}{\partial x}+v\frac{\partial C}{\partial y}=Dm\frac{\partial^2 C}{\partial y^2}-k_r(C-C_\infty). \tag{7}$$

The boundary conditions are :

$$\begin{aligned} &u=u_w=ax, v=v_w, N=-m\frac{\partial u}{\partial y}, T=T_w, C=C_w \ at \ \ y=0\\ &u\to u_\infty=bx, N\to 0, T\to T_\infty, C\to C_\infty \ \ as \ \ y\to\infty \end{aligned} \tag{8}$$

where u and v are velocity components along x and y directions, v_w, μ, ν, ρ, κ and j are suction/injection term, dynamic viscosity, kinematic viscosity, fluid density, vortex viscosity and micro inertial per unit mass respectively. Likewise, T, C, N, k, B_o and k_p are respectively the fluid temperature, concentration, component of microrotation, thermal conductivity, magnetic field intensity and permeability of the porous medium. Others are: $k_r, \sigma, C_p, p, T_w, T_\infty, C_w, C_\infty, Dm, q$ and q_r represent rate of chemical reaction, electric conductivity, specific heat at constant pressure, fluid density, temperature of the stretching plate, free stream temperature, concentration at the stretching wall and free steam concentration, molecular diffusivity, volumetric rate of heat generation and radiative heat flux respectively. Also, $F=F_0x^{-1}$ (Makinde, 2010) is a Forchheimer constant and F_0 is a constant, m is a surface boundary parameter with $0\le m\le 1$. The case when $m=0$ corresponds to $N=0$, this represents a strong concentration of the microelements, such that the micro-particles close to the wall are unable to rotate. When $m=\frac{1}{2}$, this indicates weak concentration of micro-particles and the vanishing of anti-symmetric part of the stress tensor and the case when $m=1$ is used for modelling turbulent boundary layer flows (see Peddieson , 1972; Ahmadi, 1976; Jena and Mathur, 1981).

$$k=k_\infty\left[b_1+b_2(T-T_\infty)\right] \tag{9}$$

is the temperature dependent thermal conductivity, (Mukhopahyay *et al.*, 2005), where k_∞ is

the constant value of the coefficient of thermal conductivity in the free stream. b_1 and b_2 are constants while b_2 depending on the nature of the fluid. For fluids such as air and liquids as water, $b_2 > 0$ while $b_2 < 0$ for fluids such as lubricating oils. A case where $b_1 = 1$ is investigated in this study.

$\gamma = \left(\mu + \frac{\kappa}{2}\right) j$, is the spin gradient viscosity $j = \frac{\nu}{a}$, is the micro-inertia per unit mass. This assumption has been invoked to allow the field of equations to predict the correct behaviour in the limiting case when the microstructure effects become negligible and the total spin N reduces to the angular velocity (Ahmadi, 1976).

Using Rosseland approximation,

$$q_r = -\frac{4\sigma^\star}{3\alpha^\star}\frac{\partial T^4}{\partial y}, \tag{10}$$

is the radiative heat flux (Akinbobola and Okoya, 2015; Adeniyan, 2015).

Assuming that there exists sufficiently small temperature difference within the flow such that T^4 can be expressed as a linear combination of the temperature. Expanding T^4 in Taylor series about T_∞ to get

$$T^4 = T_\infty^4 + 4T_\infty^3(T - T_\infty) + 6T_\infty^2(T - T_\infty)^2 + \ldots \tag{11}$$

neglecting higher order terms in (11) gives

$$T^4 = 4T_\infty^3 T - 3T_\infty^4, \tag{12}$$

substituting (12) in (10) to obtain

$$q_r = -\frac{16\sigma^\star T_\infty^3}{3\alpha^\star}\frac{\partial T}{\partial y}, \tag{13}$$

and differentiating (13) w. r. t. y gives

$$\frac{\partial q_r}{\partial y} = -\frac{16\sigma^\star T_\infty^3}{3\alpha^\star}\frac{\partial T^2}{\partial y^2}. \tag{14}$$

where $\alpha^\star$ is the mean absorption coefficient and $\sigma^\star$ is the Stefan-Boltzman constant. Introducing the stream function

$\psi(x, y)$ as $u = \frac{\partial \psi}{\partial y}$, $v = -\frac{\partial \psi}{\partial x}$, equation (1) is automatically satisfied.

Following Hayat *et al*, (2011) and Olajuwon *et al*, (2014), we also introduce the following dimensionless variables into eqs. (3-5)

$$\psi = xf(\eta)\sqrt{a\nu}, \eta = \sqrt{\frac{a}{\nu}}y, N = xg(\eta)\sqrt{\frac{a^3}{\nu}}, \theta = \frac{T - T_\infty}{T_w - T_\infty}, \phi = \frac{C - C_\infty}{C_w - C_\infty}. \tag{15}$$

Therefore, the resulting non-linear ODEs are:

$$(1+K)f''' + ff'' - f'^2 + \lambda^2 + Kg' - M(f' - \lambda) - Da(f' - \lambda) - Fs(f'^2 - \lambda^2) = 0, \tag{16}$$

$$(1 + K/2)g'' + fg' - f'g - K(2g + f'') = 0, \tag{17}$$

$$\left(1 + h\theta + \frac{4}{3}R\right)\theta'' + h\theta'^2 + PrEc(1+K)f''^2 + Prf\theta' + PrQ\theta = 0, \tag{18}$$

$$\phi'' + Scf\phi' - Sc\tau\phi = 0. \tag{19}$$

The corresponding boundary conditions become

$$\eta = 0 : f' = 1,\ f = fw,\ g = -mf'',\ \theta = 1,\ \phi = 1 \tag{20}$$

$$\eta \to \infty : f' = \lambda,\ g \to 0,\ \theta \to 0,\ \phi \to 0\,. \tag{21}$$

Here, prime denotes differentiation with respect toη, $K = \kappa\ /\mu$ is the material parameter, $fw = -\frac{vw}{\sqrt{av}}$ with $fw > 0$ as the suction and $fw < 0$ corresponds to injection. $Da = v/aK_p$ is the Darcy parameter, $Sc = v/Dm$ is the Schmidt number, $Q = \dfrac{q}{a\rho Cp}$ is the heat generation/absorption parameter, $Fs = \dfrac{F_0}{k_p}$ is the local Forchheimer number, $Ec = \dfrac{u_w^2}{Cp(T_w - T_\infty)}$ is the Eckert number, $R = \dfrac{4\sigma^\star T_\infty^3}{\alpha^\star k_\infty}$ is the radiation parameter, $h = b_2(T_w - T_\infty)$ is the thermal conductivity parameter, $\lambda = \dfrac{b}{a}$ is the stretching parameter and $\tau = \dfrac{k_r}{a}$ is the chemical reaction parameter.

Physical quantities of Engineering interest

The physical quantities of engineering interest in this study are the non-dimensional skin friction, rate of heat transfer, rate of mass transfer and the wall couple stress. These are respectively defined as:

$$Cf = \frac{\tau_w}{\rho u_w \sqrt{\dfrac{a}{\nu}}},\ Cs = \frac{xM_w}{\mu j u_w},\ Nu = \frac{xq_w}{k_\infty(T_w - T_\infty)},\ Sh = \frac{xq_m}{Dm(C_w - C_\infty)}, \tag{22}$$

where

$$\tau_w = \left[(\mu + \kappa)\frac{\partial u}{\partial y} + \kappa N\right]_{y=0},\ M_w = \left[\gamma \frac{\partial N}{\partial y}\right]_{y=0},\ q_w = -k\left[\frac{\partial T}{\partial y}\right]_{y=0},\ q_m = Dm\left[\frac{\partial T}{\partial y}\right]_{y=0} \tag{23}$$

are the wall shear stress, the wall couple stress, the heat flux and the mass flux respectively.

3. Method of solution

The system of non-linear ordinary differential equations $(16-19)$ together with the boundary conditions $(20-21)$ are solved numerically using shooting method alongside the fourth order Runge-Kutta integration scheme. Systematic estimate of $f''(0)$ and $\theta'(0)$ are carried out with shooting technique until the boundary conditions at infinity decay exponentially to zero.

The iteration process is repeated until the convergence criterion for all the variables at 10^{-7} is achieved. The step size $\nabla\eta = 0.001$ is used for the numerical solution, the boundary condition $\eta \to \infty$ is approximated by $\eta_{max} = 8$.

Table 1: Comparison of skin-friction coefficient $f''(0)$ for different values of λ, $Pr = 0.05$.

λ	Pop *et al.* (2004)	Mahapatra & Gupta (2002)	Ibrahim & Suneetha (2015)	Present Results
0.1	-0.9694	-0.9694	-0.9969385	-0.9693875
0.2	-0.9181	-0.9181	-0.9181065	-0.9181072
0.5	-0.6673	-0.6673	-0.6672610	-0.6672637

2.0	2.0174	2.0175	2.01744904	2.0175028

Table 2: Values of $-f''(0), -\theta'^{(0)}, -\phi'(0)$ and $-g'(0)$ for variations in $K \;\; M, fw, \tau, Pr, R, Da$ and λ

PP	Variations	$-f''(0)$	$-\theta'(0)$	$-\phi'(0)$	$-g'(0)$
K	0.00	1.7211204	0.5651760	0.4234420	1.4192105
	1.00	1.3148192	0.5329124	0.4335286	0.8654967
	2.00	1.0986491	0.48599091	0.4415668	0.6148714
M	0.00	1.2764982	0.5415542	0.4349504	0.8360854
	1.00	1.4542938	0.5022841	0.4288191	0.9732535
	2.50	1.6749555	0.4562866	0.4226206	1.1456047
fw	-0.75	0.8286034	0.1074978	0.2034698	0.2867982
	-0.40	0.9083250	0.0059069	0.2411975	0.3587369
	0.00	1.0102270	-0.1330753	0.2896861	0.4638887
	0.40	1.1237080	-0.2867262	0.3435899	0.5983277
τ	0.01	1.3148192	0.5876627	0.4023286	0.5876627
	0.10	1.3148192	0.5329124	0.4335286	0.5329124
	0.30	1.3148192	0.5329124	0.4950932	0.5329124
Pr	0.72	1.3148192	0.5329124	0.4335286	0.8654967
	1.50	1.3148192	1.0341174	0.4335286	0.8654967
	3.50	1.3148192	2.2070213	0.4335286	0.8654967
R	0.10	1.3148192	0.5851065	0.9121206	0.5994535
	0.50	1.3148192	0.4214487	0.8817577	0.6513150
	1.00	1.3148192	0.3157440	0.8663495	0.6790584
Da	0.50	1.3148192	0.3323109	0.4335286	0.8654967
	1.50	1.4863522	0.3076034	0.4278305	0.9981626
	2.50	1.6340428	0.2875696	0.4236697	1.1135020
λ	0.10	1.4251742	0.4637127	0.4162417	0.9205961
	0.30	1.1902531	0.5955953	0.4501116	0.7980220
	1.00	0.0000000	0.8740115	0.5474481	0.0000000
	1.20	-0.4248756	0.8951163	0.5708352	-0.3278221
	1.40	-0.8818353	0.8857545	0.5928892	-0.6983784

4. Results and Discussion

In order to have clear insight into the behaviour of each of the flow parameters on the physical problem, a computational analysis has been carried out for the dimensionless velocity, temperature, concentration and microrotation.

The default values for the computation are $M = 0.2, K = 1, Ec = 0.2, Pr = 0.72, Sc = 0.22, R = 0.5, \lambda = 0.2, Da = 0.5, Fs = 0.5, Q = 0.2, m = 0.5$ and $fw = 1$. The plotted graphs correspond to these values unless otherwise stated on the graph.

In the absence of micropolar parameter K, Forchheimer number Fs, suction/injection parameter fw, Eckert number Ec, chemical reaction parameter τ, and taking $Pr = 0.05$, the results have been compared with previous published results as shown in Table 1. The comparisons are found

to be in excellent agreement.

Table 2 shows the numerical values of skin friction coefficient $f''(0)$, Nusselt number $-\theta'(0)$, Sherwood number $-\phi'(0)$ and the wall couple stress $g'(0)$. Observation reveals that the material parameter K reduces the skin friction coefficient $f''(0)$, rate of heat transfer $-\theta'(0)$ and the wall couple stress $g'(0)$ but it increases $-\phi'(0)$. It is further noticed that the skin friction coefficient rises with an increase in M, fw and Da whereas the rate of heat transfer $-\theta'(0)$ falls with an increase in M, fw, R and Da. The rate of heat transfer $-\theta'(0)$ increases with a rise in Prandtl number Pr.

Fig. 2 describes the influence of magnetic field parameter M on the velocity profiles. The velocity profiles decrease with an increase in the value of the magnetic field parameter M due to the imposition of the transverse magnetic field on an electrically conducting fluid. In such situations, the magnetic field induces a retarding force known as Lorentz force which acts against the fluid motion and slows it down. In consequence of the resistance to the fluid motion caused by the this force, the micropolar fluid temperature increases as shown in Fig. 3. The microrotation component rises near the plate with an increase in the magnetic parameter M as shown in Fig. 4

Fig. 5 shows the variation of the dimensionless velocity with η for different values of material (micropolar) parameter K. It is observed that the velocity profiles increase with an increase in K due to the rising in the boundary layer thickness. In addition, the velocity in case of micropolar fluid is higher than that of viscous fluid (*i.e.* $K = 0$). Fig. 6 shows that the microrotation profiles decrease near the plate, whereas further from the plate opposite is the case. The effects of Darcy parameter *Da* and Forchheimer *Fs* on the velocity distribution are depicted in Figs. 7 and 8. The fluid velocity decreases for both *Da* and *Fs*, this response is due to the fact that the porous medium creates a resistance against the fluid flow which results from decreasing porosity of the porous medium. This agrees well with Ibrahim and Suneetha (2015).

Fig. 9 depicts the influence of the stretching parameter λ on the velocity distribution in the boundary layer. λ describes the ratio of the free stream velocity to that of the stretching velocity. Two sets of values of λ are examined $\lambda < 1$ and $\lambda > 1$. It is evident from Fig. 9 that the fluid velocity increases with an increase in the magnitude of λ in both cases. When $\lambda > 1$, the free stream accelerates faster than the stretching velocity and there exist a boundary layer structure. This causes an increase in pressure and straining motion near the stagnation point leading to the shrinking of the boundary layer thickness. However, when $\lambda < 1$, the flow has an inverted boundary layer structure and no formation of the boundary layer structure when $\lambda = 1$. Figs. 10 -11 display the variation of the wall temperature and concentration with η for different values of λ. Observation shows that both the wall temperature and concentration fall with a rise in λ for both and $\lambda > 1$ and $\lambda < 1$ due to decrease in the thermal and solutal boundary layer thicknesses.

Fig. 12-14 describe the variation of the velocity, temperature and concentration with η for different values of suction/injection parameter fw. There is a decrease in velocity, temperature and concentration profiles with an increase in fw as noticed. The response is due to the fact that momentum boundary layer thickness decreases with a rise in suction velocity. Moreso, $fw > 0$ creates a damping effect on the flow field which is due the fact that the heated fluid is being pushed towards the plate and the buoyancy force acts to retard the fluid as a result of high influence of viscosity. On the other hand, injection parameter $fw < 0$ enhances velocity distribution within the boundary layer.

Fig. 15 depicts the variation of temperature with η for different values of Eckert number Ec.

Eckert number describes the ratio of kinetic energy of the flow to the boundary layer enthalpy difference, that is, the conversion of kinetic energy into thermal energy by the work done against the viscous fluid stresses. An increase in Ec causes the fluid temperature to rise more than the surface temperature. Fig. 16 shows that an increase in the radiation parameter R enhances the temperature distribution across the boundary layer. Physically, an increase in R has the tendency to increase the conduction effects leading to a rise in temperature at every point away from the plate.

Fig. 17 illustrates the influence of Prandtl number Pr on the temperature profiles. Increase in Pr causes a reduction in the temperature profiles. Physically, Prandtl number expresses the ratio of momentum diffusivity to thermal diffusivity and it controls the relative thickness of the momentum and thermal boundary layers. Thus, increasing Pr implies reducing thermal boundary layer thickness which in turn lowers the average temperature within the boundary layer. Prandtl parameter Pr can therefore be used to enhance the rate of cooling as fluids with moderate Pr creates higher conductivities and such heat diffuses quickly away from the heated plate than for higher values of Pr .

Figs. 18 and 19 portray the effects of surface boundary parameter m on the velocity and microrotation profiles. It is observed that increasing surface boundary parameter m decreases the hydrodynamic boundary layer thickness but enhances the microrotation boundary thickness.

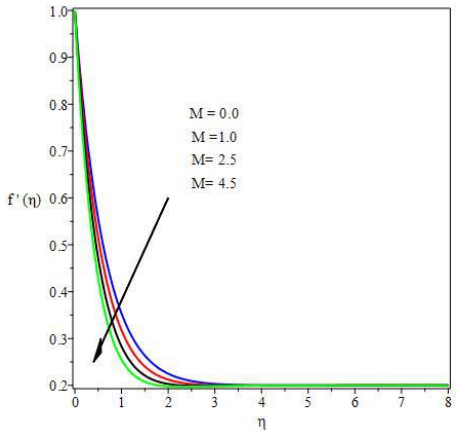

Fig. 2. Velocity profiles for different values of M

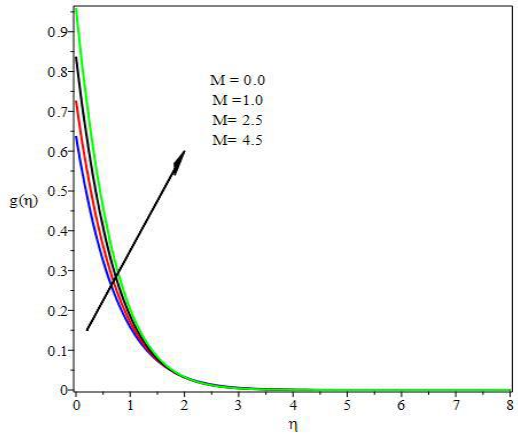

Fig. 4. microrotation profiles for different values of M

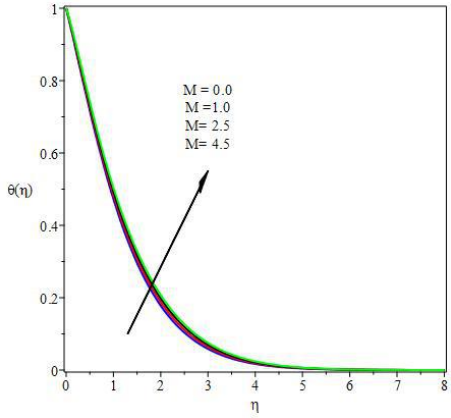

Fig. 3. temperature profiles for different values of M

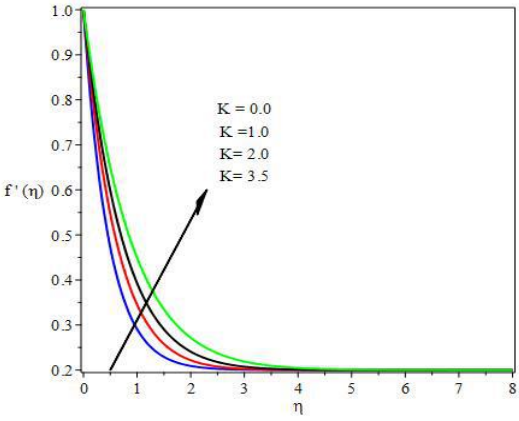

Fig. 5. velocity profiles for different values of K

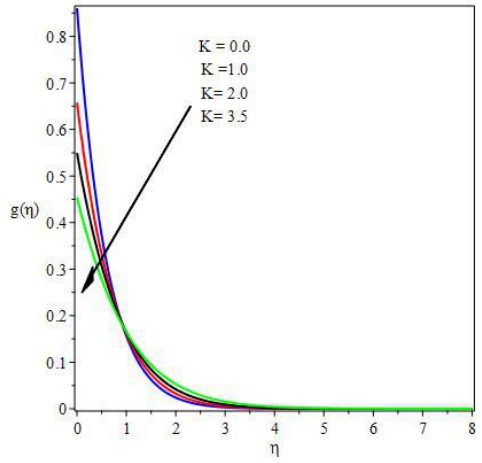

Fig .6. Microrotation profiles for different values of *K*

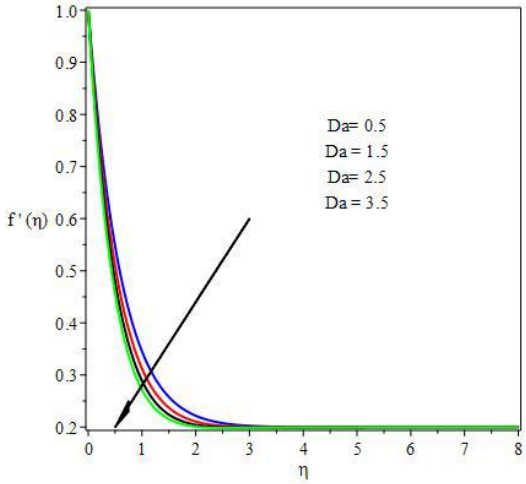

Fig. 7. velocity profiles for different values of *Da*

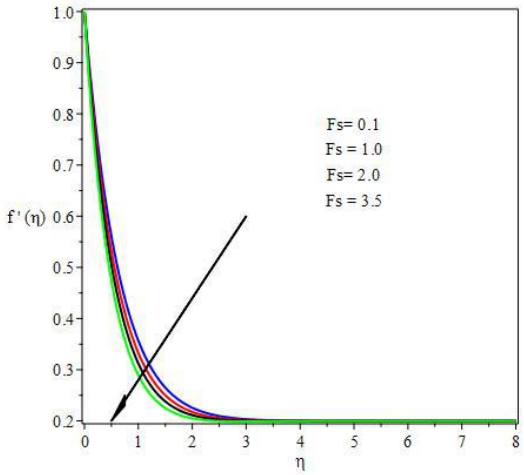

Fig. 8. velocity profiles for different values of *Fs*

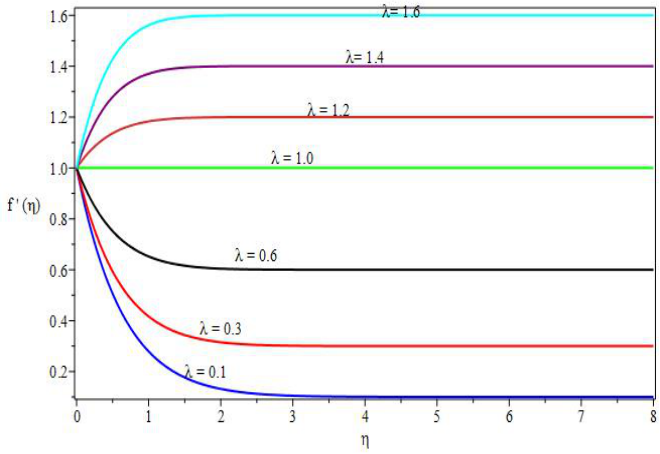

Fig. 9. velocity profiles for different values of λ

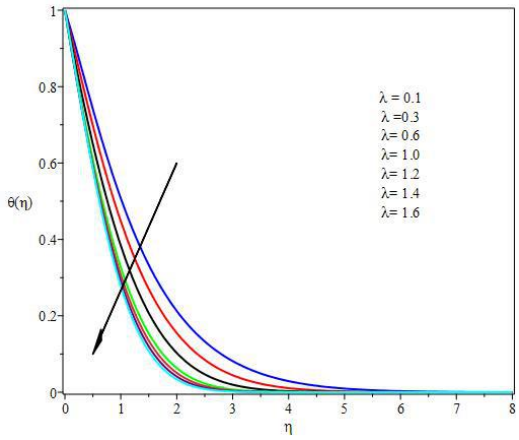

Fig. 10. temperature profiles for different values of λ

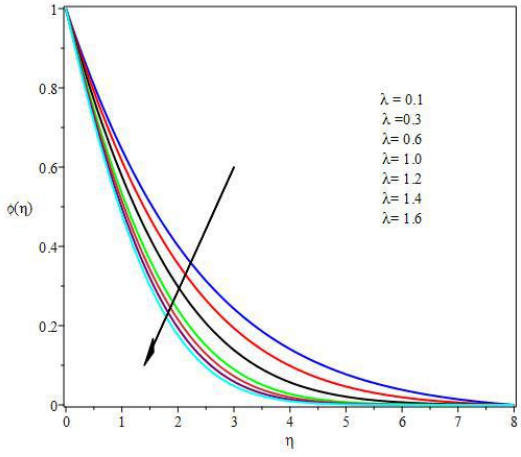

Fig. 11. Concentration profiles for different values of λ

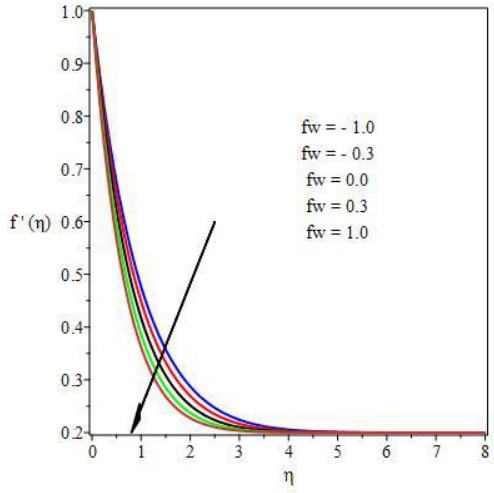

Fig.12. velocity profiles for different values of *fw*

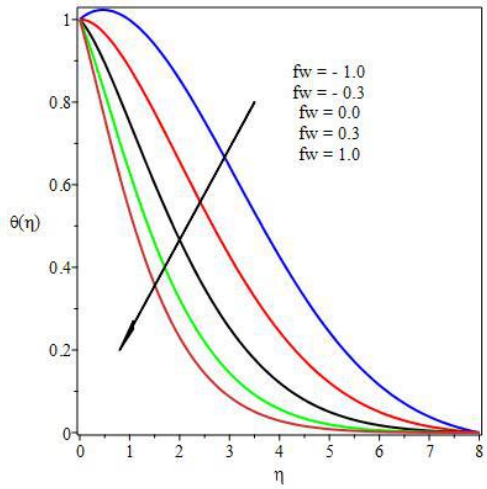

Fig. 13. temperature profiles for different values of *fw*

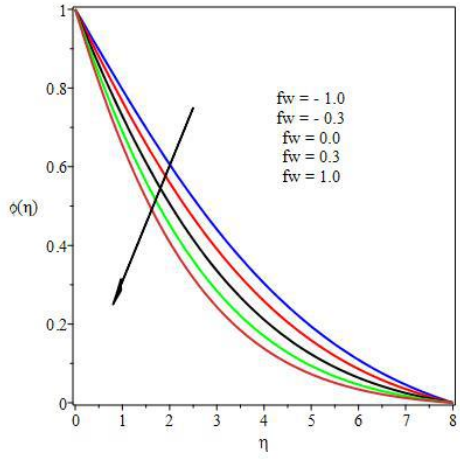

Fig. 14. Concentration profiles for different values of *fw*

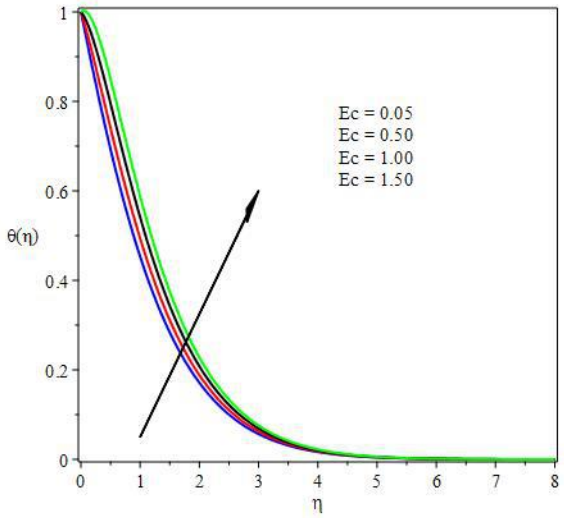

Fig.15. temperature profiles for different values of *Ec*

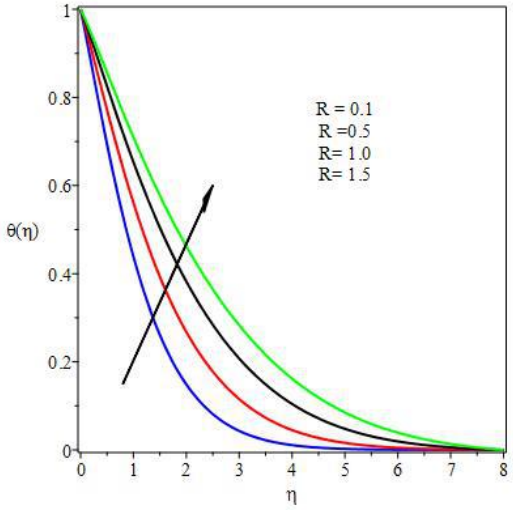

Fig. 16. temperature profiles for different values of *R*

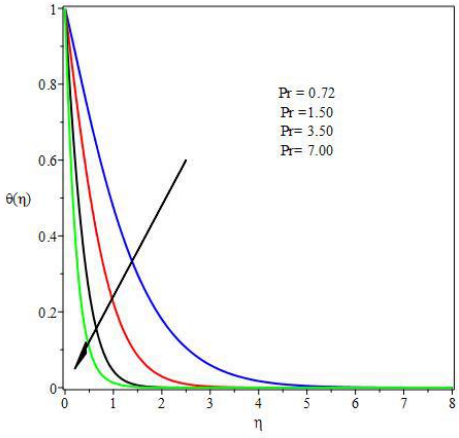

Fig. 17. temperature profiles for different values of *Pr*

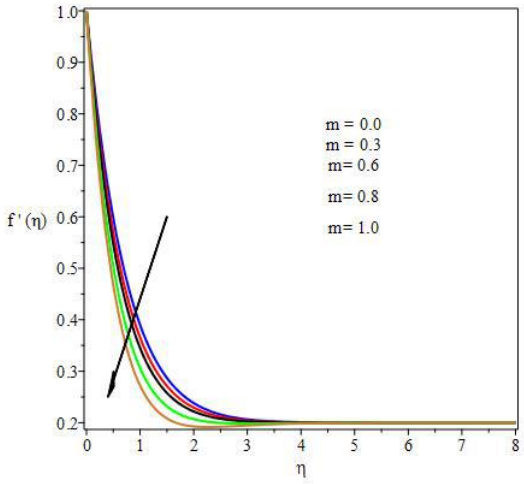

Fig.18. velocity profiles for different values of m

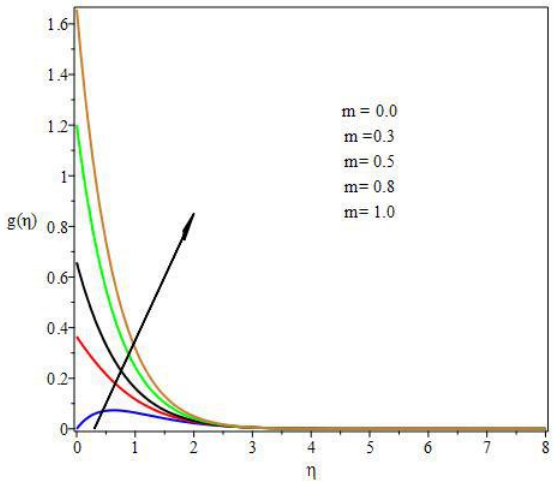

Fig.19. microrotation profiles for different values of m

5. Conclusion

The present study numerically investigates the MHD stagnation-point flow of a micropolar fluid past linearly stretching sheet in a saturated porous medium. The governing PDEs of the fluid flow are transformed into non-linear ODEs using similarity variables. Shooting method is used to solve the non-linear system of equations alongside the fourth order Runge-Kutta integration scheme. The influences of the physical parameters on the dimensionless velocity, temperature, concentration and microrotation profiles have been found. Similarly, the effects of pertinent flow parameters on the skin friction cofficient $f''(0)$, Nusselt number $-\theta(0)$, Sherwood number $-\phi(0)$ and the wall couple stress $g'(0)$ are computed and presented in a table. The following conclusions are drawn from the study:

- The material (micropolar) parameter K causes an increase in the fluid velocity while decreasing the microrotation near the plate. In addition, the influence of K is to decrease the skin friction coefficient $f''(0)$, heat transfer $\theta'(0)$ and wall couple stress $g'(0)$. Thus, K can be useful in reducing drag along the plate.
- An increase in the magnetic parameter M decreases velocity, heat and mass transfer but increases temperature, microrotation, skin friction coefficient, and wall couple stress.
- An increase in the stretching parameter λ causes a rise in the velocity for both $\lambda > 1$ and $\lambda < 1$ with no formation of boundary layer structure when $\lambda = 1$. A corresponding decrease in temperature and concentration of the fluid is noticed for an increase in λ.
- An increase in the Prandtl number Pr causes a reduction in fluid temperature while enhancing the rate of heat transfer. Hence, Pr can be applied for cooling of the plate.
- Sherwood number $-\phi(0)$ is an increasing function of chemical reaction parameter τ.
- Radiation parameter R decreases Nusselt number $-\theta(0)$ while the skin friction coefficient $f''(0)$ increases with an increase in Darcy parameter Da.
- The surface boundary parameter m decreases fluid velocity while causing a rise in the microrotation of fluid constituents.

References

Adeniyan, A. (2015). MHD mixed convection of a viscous dissipating and chemically reacting stagnation-point flow near a vertical permeable plate in a porous medium with thermal radiation and heat source/sink, *Asian Journal of Mathematics and* Applications, **2015**, 1-23.

Akinbobola, T. E. and Okoya, S. S. (2015). The flow of second grade fluid over a stretching sheet with variable thermal conductivity and viscosity in the presence of heat source/sink, *Journal of Nigeria Mathematical Society*, **34**, 331-342.

Ahmadi, G. (1976). Self-similar solution of incompressible micropolar boundary layer flow over a semi-infinite plate, Int. J. Engng Sci, **14**, 639-646.

Chen, J., Liang, C. and Lee, J. D. (2011). Theory and simulation of micropolar fluid dynamics, *J. Nanoengineering and nanosystems*, **224**, 31-39.

Crane, L. J. (1970). Flow past a stretching plate, *Communicatios Breves*, **21**, 645-647.

Dar, A. A. and Elangovan, K. (2016). Thermal diffusion, radiation and inclined magnetic field effects on oscillatory flow in an asymmetric channel in presence of heat source and chemical reaction, *Journal of Nigerian Mathematical Society*, **35**(3), 488-509.

Dar, A. A. and Elangovan, K. (2017). Inclined magnetic field and thermal radiation effect on electroosmotic flow of a micropolar fluid through a porous micro-channel, *Journal of Advanced Mathematics and Applications*, **6**, 112.

Eringen, A. C. (1966). Theory of micropolar fluids, *J. Math. Anal. Appl.*, **16**, 1-18.

Eringen, A. C. (1972). Theory of thermo-microfluids, *Journal of Mathematical Analysis* and Applications, **38**, 480-496.

Gupta, P. S. and Gupta, A. S. (1977). Heat and mass transfer on a stretching sheet with suction or blowing, *Can. J. Chem. Eng.*, **55**, 744-746

Hayat, T., Mustafa, M. and Obaidat, S. (2011). Soret and Dufour effects on the stagnation-point flow of a micropolar fluid toward a stretching sheet, *Journal of Fluid* Engineering, **133**, 1-9.

Hayat, T., Shehzda, S. A. and Qasim, M. (2011). Mixed convection flow of a micropolar fluid with radiation and chemical reaction, *Int., Journal for Numerical Methods in* 14 *Fluids*, **67**, 1418-1436.

Hoyt, J. W. and Fabula, A. G. (1970). *The Effects of Additives on Fluid Friction*, US Naval Ordinance Test Station Report.

Ibrahim, S. M and Suneetha (2015). Effects of heat generation and thermal radiation on steady MHD flow near a stagnation point on a linear stretching sheet in porous medium, *Journal of Computational and applied Research in Mechanical Engineering*, **4**, 133-144.

Jat, R. N, Saxena, V. and Rajotia, D. (2012). MHD stagnation point flow and heat transfer of a micropolar fluid in a porous medium, *Journal of International* Academy Physical Sciences, **16**, 315-328

Jena, S. K. and Mathur, M. N. (1981). Similarity solutions for laminar free convection flow of a thermomicropolar fluid past a non-isothermal flat plate, International J. Eng. Sci. **19**, 1431-1439.

Khan, S. U., Ali, N. and Abbas, Z. (2015). Hydromagnetic flow and heat transfer over a porous oscillating stretching surface in a viscoelastic fluid with porous medium, *Plos One*, **10**(12), 1-18.

Lukaszewicz, G. (1999). *Micropolar fluids: Theory and Applications* 1st Ed., Birkhauser, Boston.

Mahapatra, T. R. and Gupta, A. S. (2002). Heat transfer in stagnation point flow towards a stretching sheet, *Heat and Mass Transfer*, **38,** 517-521.

Mahmoud, M. A. A. (2011). Hydrodynamic stagnation point flow towards a porous stretching sheet with variable surface heat flux in the presence of heat generation, *Chem. Eng. Comm.*, **198**, 837-846.

Makinde, O. D. (2010). Similarity solution of hydromagnetic heat and mass transfer over a vertical plate with a convective surface boundary condition, *Int. Journal of the Physical Sciences*, **5**, 700-710.

Mishra, S .R, Baag, S.& Mohapatra, D. K. Chemical reaction and Soret effects on hydromagnetic micropolar fluid along a stretching sheet, *Engineering Science and Technology, an Int.* Journal, **19**, 1919-1928.

Mukhopadhyay, S., Layek, G. C. and Samad S. A. (2005). Study of MHD boundary layer flow over a heated stretching sheet with variable viscosity, International *Journal of* Heat and Mass Transfer, **48**, 4460-4466.

Mukhopadhyay, S. (2013). Effects of thermal radiation and variable fluid viscosity on stagnation point flow past a porous stretching sheet, *Meccanica*, **48**, 1717-1730.

Olajuwon, B. I., Oahimire, J. I. and Waheed, M. A. (2014). Convection heat and mass transfer in a hydromagnetic flow of a micropolar fluid over a porous medium, *Theoret. Appl. Mech*, **41**, 93-117.

Pal, D. and Chatterjee, S. (2010). Heat and mass transfer in MHD non-Darcian flow of a micropolar fluid over a stretching sheet embedded in a porous media with non-uniform heat source and thermal radiation, *Commun Nonlinear Sci. Numer* Simulat, **15**, 1843-1857.

Pandey, A. K and Kumar, M. (2016). Effect of viscous dissipation and suction/injection on MHD nano fluid flow over a wedge with porous medium and slip, *Alexandria* 15 *Engineering Journal*, **55**(4), 31153123.

Peddieson, J and McNitt, R. P. (1970). Boundary layer theory for micropolar fluid, *Recent Adv. Enggng Sci.*, **5**, 405.

Peddieson, J. (1972). An application of the micropolar model to the calculation of a turbulent shear flow, *Int. J. Eng. Sci,* **10**, 23-32.

Pop, S. R., Grosan, T. and I. Pop, (2004). Radiation effect on the flow near the stagnation point of a stretching sheet, *Technische Mechanik*, **25**, 100-106.

Vogel, W. A. and Patterson, A. M. (1964). *An Experimental Investigation of Additives* Injected into the Boundary Layer of an Underwater Body, Pacific Naval Lab. of the Defense Res. Board of Canada, Report.

Wilson, A. J. (1970). Boundary layers in micropolar liquids, *Proceedings of Cambridge* Philosophical society, **67**, 469-470.